THE ASTROPHYSICAL JOURNAL, 558:L93–L96, 2001 September 10

STRONG EVIDENCE FOR A BURIED ACTIVE GALACTIC NUCLEUS IN UGC 5101: IMPLICATIONS FOR LINER-TYPE ULTRALUMINOUS INFRARED GALAXIES

MASATOSHI IMANISHI[1]
National Astronomical Observatory, Osawa 2-21-1, Mitaka, Tokyo 181-8588, Japan; imanishi@optik.mtk.nao.ac.jp
C. C. DUDLEY[2]
Naval Research Laboratory, Remote Sensing Division, Code 7217, Building 2, Room 240B, 4555 Overlook Avenue, SW, Washington, DC 20375-5351; dudley@vivaldi.nrl.navy.mil
AND
PHILIP R. MALONEY
Center for Astrophysics and Space Astronomy, University of Colorado, Campus Box 389, Boulder, CO 80309-0839; maloney@casasrv.colorado.edu
Received 2001 June 21; accepted 2001 August 3; published 2001 August 16

ABSTRACT

We report on the results of 3–4 μm spectroscopy of the ultraluminous infrared galaxy (ULIRG) UGC 5101. It has a cool far-infrared color and a LINER-type optical spectrum and so, based on a view gaining some currency, would be regarded as dominated by star formation. However, we find that it has strong 3.4 μm carbonaceous dust absorption, low equivalent width 3.3 μm polycyclic aromatic hydrocarbon (PAH) emission, and a small 3.3 μm PAH–to–far-infrared luminosity ratio. This favors an alternative scenario, in which an energetically dominant active galactic nucleus (AGN) is present behind obscuring dust. The AGN is plausibly obscured along all lines of sight (a "buried AGN") rather than merely obscured along our particular line of sight. Such buried AGNs have previously been found in thermal infrared studies of the ULIRGs IRAS 08572+3915 and IRAS F00183−7111, both classified optically as LINERs. We argue that buried AGNs can produce LINER-type optical spectra and that at least some fraction of LINER-type ULIRGs are predominantly powered by buried AGNs.

Subject headings: galaxies: active — galaxies: individual (UGC 5101) — galaxies: nuclei — infrared: galaxies

1. INTRODUCTION

Ultraluminous infrared galaxies (ULIRGs) radiate most of their extremely large, quasar-like luminosities ($>10^{12}\ L_{\odot}$) as infrared dust emission and dominate the bright end of the galaxy luminosity function in the nearby universe (Soifer et al. 1987). Recent studies have revealed that the bulk of the cosmic submillimeter background emission has been resolved into discrete sources, similar to nearby ULIRGs (Blain et al. 1999a), and for this reason, data on nearby ULIRGs have been extensively used to derive information on star formation rates, dust content, and metallicity in the early universe (Barger, Cowie, & Richards 2000; Blain et al. 1999b). Understanding the nature of nearby ULIRGs is therefore of particular importance both locally and cosmologically.

In contrast to the majority of less infrared luminous ($<10^{12}\ L_{\odot}$) galaxies, it has been suggested that energetically important, dust-obscured active galactic nuclei (AGNs) are present in ULIRGs (Veilleux, Kim, & Sanders 1999a; Fischer 2000). If the geometry of the dust distribution is toroidal and/or the amount of dust along our line of sight is not too great, signatures of such dust-obscured AGNs can be found in the optical and/or near-infrared wavelength range at $\lambda < 2$ μm (Veilleux et al. 1999a; Veilleux, Sanders, & Kim 1999b). However, detecting AGNs that are deeply embedded in a spherical dust shell (hereafter buried AGNs) and estimating their energetic importance is very difficult at $\lambda < 2$ μm, even though they are energetically important, since spectral tracers are dominated by less strongly obscured star formation activity. To detect such buried AGNs and estimate their energetic importance, we must observe at wavelengths where the effects of dust extinction are smaller.

At wavelengths 3–13 μm, dust extinction is lower. Furthermore, emission is dominated by radiation from dust, the dominant emission mechanism of ULIRGs. Thus, discussions of the energy sources of ULIRGs are more straightforward than those based on observations at X-ray or radio wavelengths, which are also potentially capable of detecting buried AGNs, but are dominated by emission mechanisms other than dust emission. Finally, by using spectral features at 3–13 μm, we can distinguish the energy sources of individual galaxies: while star formation–dominated galaxies show strong polycyclic aromatic hydrocarbon (PAH) emission features, buried AGNs should show dust absorption features below smooth continuum emission (Roche et al. 1991; Genzel et al. 1998; Dudley 1999; Imanishi & Dudley 2000). Using spectral features, particularly the 7.7 μm PAH emission, in the rest-frame 5–11 μm spectra obtained with the *Infrared Space Observatory* (*ISO*), it has been argued that the majority of ULIRGs are star formation–powered (Genzel et al. 1998; Rigopoulou et al. 1999; Tran et al. 2001). However, the determination of the continuum level with respect to which emission and absorption features should be measured in *ISO* spectra is highly uncertain due to insufficient wavelength coverage longward of these features. Distinguishing between star formation and buried AGN activity therefore remains controversial (Dudley 1999; Spoon et al. 2001).

As discussed in Imanishi & Dudley (2000), observations at 3–4 μm have two important advantages: first, dust extinction is as small as that at 7–8 μm (Lutz et al. 1996); and second, the 3.3 μm PAH emission and 3.4 μm carbonaceous dust absorption features can be used to distinguish between the different energy sources of ULIRGs, without serious uncertainty in the continuum determination. Ground-based 3–4 μm spec-

[1] Visiting Astronomer at the Infrared Telescope Facility, which is operated by the University of Hawaii under contract from the National Aeronautics and Space Administration.
[2] NRL/NRC Research Associate.

TABLE 1
SUMMARY OF UGC 5101, IRAS 08572+3915, AND IRAS F00183−7111

Object	Redshift	f_{25}[a] (Jy)	f_{60}[a] (Jy)	f_{100}[a] (Jy)	log L_{FIR}[b] (ergs s^{-1})	f_{25}/f_{60}[c]
UGC 5101	0.040	1.03	11.54	20.23	45.61	0.09 (cool)
IRAS 08572+3915	0.058	1.70	7.43	4.59	45.62	0.23 (warm)
IRAS F00183−7111	0.327	0.13	1.20	1.19	46.51	0.11 (cool)

[a] The f_{25}, f_{60}, and f_{100} are *IRAS* FSC fluxes at 25, 60, and 100 μm, respectively.
[b] Logarithm of far-infrared (40–500 μm) luminosity in units of ergs per second calculated with $L_{FIR} = 1.4 \times 2.1 \times 10^{39} D$ (Mpc)^2 × (2.58$f_{60} + f_{100}$) ergs s^{-1} (Sanders & Mirabel 1996).
[c] Objects with $f_{25}/f_{60} <$ (>)0.2 are called cool (warm) (Sanders et al. 1988b).

troscopy is thus potentially a powerful tool to investigate the energetic importance of AGNs buried in the compact nuclei of ULIRGs and to settle the controversy discussed above. Our particular interest is the search for buried AGNs in ULIRGs with cool far-infrared colors and/or non-Seyfert optical spectra, which are typically taken to be star formation–dominated, based on *ISO* studies (Genzel & Cesarsky 2000; Taniguchi et al. 1999; Lutz, Veilleux, & Genzel 1999). UGC 5101 is such a ULIRG (Table 1; Veilleux et al. 1999a) and has actually been diagnosed as being star formation–powered (Rigopoulou et al. 1999). In this Letter, we report on the results of 3–4 μm spectroscopic observations of UGC 5101 and the discovery of evidence for an energetically important buried AGN in this source. Throughout this Letter, $H_0 = 75$ km s^{-1} Mpc^{-1}, $\Omega_M = 0.3$, and $\Omega_\Lambda = 0.7$ are adopted.

2. OBSERVATIONS AND DATA ANALYSIS

We used the NSFCAM grism mode (Shure et al. 1994) to obtain a 3–4 μm spectrum of UGC 5101 at the Infrared Telescope Facility on Mauna Kea, Hawaii, on the night of 2001 April 9 (UT). Sky conditions were photometric throughout the observations, and the seeing was measured to be 0.″7–0.″8 FWHM. The detector was a 256 × 256 InSb array. The *HKL* grism and *L* blocker were used with the 4 pixel slit (=1.″2). The resulting spectral resolution was ~150 at 3.5 μm.

The spectrum of UGC 5101 was obtained toward the flux peak at 3–4 μm. The position angle of the slit was 0° east of north. A standard telescope nodding technique with a throw of 12″ was employed along the slit to subtract background emission. HR 4112 (F8 V, $V = 4.8$) was observed with an air-mass difference of less than 0.1 to correct for the transmission of the Earth's atmosphere and provide flux calibration.

Standard data analysis procedures were employed, using IRAF.[3] Initially, bad pixels were replaced with the interpolated signals of the surrounding pixels. Bias was subsequently subtracted from the obtained frames, and the frames were divided by a spectroscopic flat frame. Finally, the spectra of UGC 5101 and HR 4112 were extracted. Wavelength calibration was performed taking into account the wavelength-dependent transmission of the Earth's atmosphere. Since we set each exposure time to 1.2 s for the UGC 5101 observation, to reduce observing overheads, data at greater than 4 μm were affected by the nonlinear response of the detector. We excluded these data from our analysis. The UGC 5101 spectrum was then divided by the observed spectrum of HR 4112 and multiplied by the spectrum of a blackbody with a temperature appropriate to F8 V stars (6200 K). By adopting $L = 3.4$ for HR 4112 based on $V-L = 1.4$ (Tokunaga 2000), a flux-calibrated spectrum was produced.

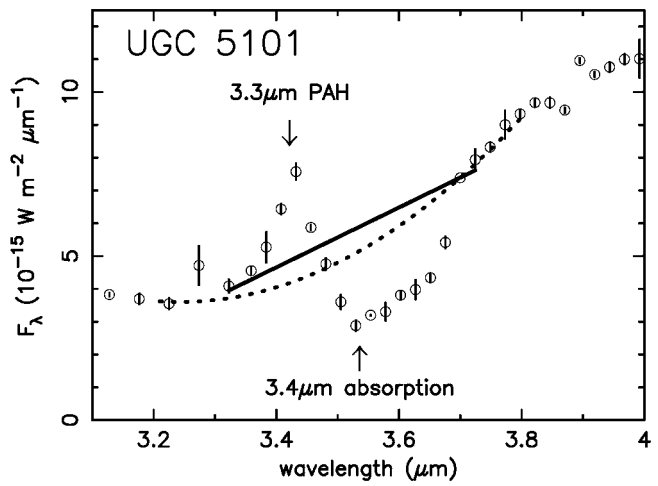

FIG. 1.—The 3–4 μm spectrum of UGC 5101. The abscissa and ordinate are the observed wavelength and the flux in F_λ, respectively. The solid and dashed lines are possible continuum levels (see § 3).

3. RESULTS

A flux-calibrated 3–4 μm spectrum of UGC 5101 is shown in Figure 1. At 3–4 μm, UGC 5101 was spatially very compact, and its spatial extent along the slit direction was indistinguishable from a point source. The spatially unresolved red near-infrared nucleus reported by Scoville et al. (2000) and interpreted as a possible AGN by these authors is the probable origin of the bulk of the detected 3–4 μm continuum in our spectrum. Our spectrum gives a value of L (3.55 μm) of 10.1 mag, which is similar to the value of L' (3.7 μm) of 9.8 mag measured with a 5″ aperture (Sanders et al. 1988a). Given that UGC 5101 has a red near-infrared color ($K-L' = 1.3$; Sanders et al. 1988a), so that $L-L'$ should be greater than 0 mag, our slit loss for the continuum emission is less than 0.3 mag. The dust continuum emission at 10–20 μm (Soifer et al. 2000), Paα emission (Genzel et al. 1998, the top middle panel of Fig. 8), and 6–18 cm radio continuum emission (Sopp & Alexander 1991; Crawford et al. 1996) all show a centrally peaked morphology, with spatially extended emission presumably originating in weakly obscured star formation activity. Our 1.″2 slit covers the bulk of this emission, so that most of the PAH emission should also be covered with our slit. Any missing PAH flux is very likely to be much smaller than the detected PAH flux and will not seriously affect our

[3] IRAF is distributed by the National Optical Astronomy Observatories, which are operated by the Association of Universities for Research in Astronomy, Inc., under cooperative agreement with the National Science Foundation.

quantitative discussion of the energy source of UGC 5101 (§ 4.1).

The spectrum in Figure 1 shows a remarkable deviation at 3.3–3.7 μm from the smooth continuum emission. (A linear continuum level is shown as the solid line in Fig. 1.) We attribute the emission feature to 3.3 μm PAH emission, since the flux peak at 3.42 μm is consistent with the expected peak wavelength of the redshifted PAH emission (3.29 μm × 1.040). Based on our adopted linear continuum level, the observed flux and rest-frame equivalent width of the 3.3 μm PAH emission are estimated to be $f_{\rm PAH} = 1.3 \times 10^{-13}$ ergs s^{-1} cm^{-2} and EW$_{\rm PAH} = 0.025$ μm, respectively.

At wavelengths longward of the PAH emission, signals at 3.5–3.7 μm are suppressed compared to the continuum level. The flux level suddenly and steeply decreases at ~3.7 μm, compared to the extrapolation from longer wavelengths, so that a strong absorption feature is undoubtedly present. We attribute this flux suppression to the 3.4 μm carbonaceous dust absorption (Pendleton et al. 1994), because the observed maximum of absorption at ~3.53 μm is consistent with the redshifted absorption peak wavelength of the carbonaceous dust absorption feature (3.4 μm × 1.040). Its observed optical depth is $\tau_{3.4}$(observed) ~ 0.7.

The 3.3 μm PAH emission profile almost fades out at 3.33–3.34 μm (Tokunaga et al. 1991; Imanishi & Dudley 2000), while the 3.4 μm carbonaceous dust absorption profile is just beginning at this wavelength range (Pendleton et al. 1994). At $z = 0.040$, this wavelength range, where neither emission nor absorption is particularly important, is redshifted to 3.46–3.47 μm. It will be seen that in Figure 1 the adopted linear continuum intersects the observed data points at this wavelength, providing further evidence that the continuum determination is reasonable. An alternative hypothesis is represented by the curved continuum shown as the dashed line in Figure 1. If this model were adopted, the observed flux and rest-frame equivalent width of the 3.3 μm PAH emission would increase to $f_{\rm PAH} = 2.0 \times 10^{-13}$ ergs s^{-1} cm^{-2} and EW$_{\rm PAH} = 0.045$ μm, respectively, and the observed optical depth of the 3.4 μm dust absorption would decrease to $\tau_{3.4}$(observed) ~ 0.6. However, the level of this curved continuum seems to be too low; it requires that the absorption optical depth be close to zero at 3.48 μm, or 3.35 μm in the rest frame, where the optical depth should in fact be significant (Pendleton et al. 1994). We thus believe that the actual PAH flux and equivalent width are lower than the values inferred using the curved continuum level; we can use these latter values as stringent upper limits. Considering the uncertainty of the continuum determination, we combine the values measured based on the two continuum levels and adopt $f_{\rm PAH} = 1.6 \pm 0.3 \times 10^{-13}$ ergs s^{-1} cm^{-2}, EW$_{\rm PAH} = 0.035 \pm 0.010$ μm, and $\tau_{3.4}$(observed) $= 0.65 \pm 0.05$.

4. DISCUSSION

4.1. *A Buried AGN in UGC 5101*

The detection of 3.3 μm PAH emission indicates the presence of star formation activity. However, its observed luminosity is $(5.2 \pm 1.0) \times 10^{41}$ ergs s^{-1}, which yields an observed 3.3 μm PAH–to–far-infrared luminosity ratio (Table 1) of ~1 × 10^{-4}, an order of magnitude smaller than is found in star formation–dominated galaxies (~1 × 10^{-3}; Mouri et al. 1990). The detected, weakly obscured star formation activity thus contributes little to the huge far-infrared luminosity of UGC 5101, and a dominant energy source must be located behind the dust.

The presence of such a dust-obscured energy source is supported by the detection of strong 3.4 μm carbonaceous dust absorption. If the 3–4 μm continuum emission source behind the dust originated in star formation activity, the rest-frame equivalent width of the 3.3 μm PAH emission should be similar to those of less obscured star formation–dominated galaxies (~0.12 μm; Imanishi & Dudley 2000), because both 3–4 μm continuum and 3.3 μm PAH emission fluxes would be attenuated similarly by dust extinction. The observed rest-frame equivalent width is, however, smaller by more than a factor of 3. Consequently, the emission from behind the dust shows virtually no PAH emission, suggesting that the source is an AGN. This AGN activity dominates the observed 3–4 μm continuum flux, contributing ~70% of it, and is plausibly the energy source of UGC 5101's far-infrared luminosity. If the dust obscuring such an energetically important AGN had a torus-like geometry, we would expect UGC 5101 to be optically classified as a Seyfert 2 galaxy, but in fact the non-Seyfert optical classification of UGC 5101 (Veilleux et al. 1999a) implies that the AGN is obscured by dust along all lines of sight (that is, a buried AGN).

After subtracting the contribution from star formation to the observed 3–4 μm fluxes by using the spectral shape of the starburst galaxy NGC 253 in Imanishi & Dudley (2000), we estimate the intrinsic optical depth of the 3.4 μm carbonaceous dust absorption toward the buried AGN to be $\tau_{3.4}$(intrinsic) ~ 0.8, which yields dust extinction of $A_V >$ 100 mag if a Galactic extinction curve is assumed (Pendleton et al. 1994). Assuming $A_{3-4\,\mu{\rm m}} \sim 0.05 A_V$ (Lutz et al. 1996), we estimate the dereddened 3–4 μm dust emission luminosity powered by the buried AGN to be $\nu L_\nu \gtrsim 10^{45}$ ergs s^{-1}, which is comparable to the *observed* peak dust emission luminosity at 60 and 100 μm ($\nu L_\nu \sim 2 \times 10^{45}$ ergs s^{-1}, as calculated based on the *IRAS* fluxes shown in Table 1). In the case of a buried AGN, dust radiative transfer controls the temperature of the dust shell; the temperature of the dust decreases with increasing distance from the central AGN. The entire luminosity is transferred at each temperature. The present data thus provide evidence for an inner ~900 K, 3–4 μm continuum–emitting dust shell of a luminosity similar to that of the observed outer ~40 K, 60–100 μm continuum–emitting dust shell, as is expected from the buried AGN scenario.

For obscured AGNs, Alonso-Herrero, Ward, & Kotilainen (1997) found that the column density of X-ray–absorbing gas, parameterized by $N_{\rm H}$, relative to dust extinction toward the 3–4 μm continuum–emitting region (A_V), is often higher by a large factor than the Galactic $N_{\rm H}/A_V$ ratio (1.8×10^{21} cm^{-1} mag^{-1}; Predehl & Schmitt 1995). Dust obscuration toward the 3–4 μm continuum–emitting region around the buried AGN in UGC 5101 is so high ($A_V > 100$ mag; this work) that $N_{\rm H}$ could easily exceed 10^{24} cm^{-2}, in which case direct 2–10 keV X-ray emission from the buried AGNs would be very strongly attenuated. The nondetection of 2–10 keV X-rays from the putative buried AGN with *ASCA* (Nakagawa et al. 1999) can thus be explained without difficulty.

The radio–to–far-infrared flux ratio of UGC 5101 is a factor of 2 larger than the typical values for star formation–dominated galaxies at 1.5 GHz (Crawford et al. 1996) but inside their scatter at 151 MHz and 5 GHz (Cox et al. 1988; Sopp & Alexander 1991). Although the bulk of the radio emission is extended (Crawford et al. 1996; Sopp & Alexander 1991), the spatially unresolved VLBI radio core, interpreted as an AGN by Smith, Lonsdale, & Lonsdale (1998), is luminous enough

to account for the bolometric luminosity of UGC 5101 with AGN activity (Lonsdale, Smith, & Lonsdale 1995).

4.2. *Implications for Optically LINER-Type ULIRGs*

Besides UGC 5101, studies in the thermal infrared have provided evidence for the presence of energetically dominant buried AGNs in two other optically non-Seyfert ULIRGs, IRAS 08572+3915 (Dudley & Wynn-Williams 1997; Imanishi & Dudley 2000) and IRAS F00183−7111 (Tran et al. 2001). The far-infrared emission properties of these three ULIRGs are summarized in Table 1. In the optical, all are classified as LINERs (Veilleux et al. 1999a; Lutz et al. 1999). For ULIRGs classified optically as LINERs, which constitute ~40% of ULIRGs (Veilleux et al. 1999a), two arguments based on *ISO* studies have been made: (1) star formation activity is energetically dominant, and (2) the LINER-type optical line emission is due to superwind-driven shocks caused by star formation activity (Taniguchi et al. 1999; Lutz et al. 1999). The first argument, however, is not applicable to the three ULIRGs in Table 1. Then what is the origin of the LINER-type optical emission in these objects?

In buried AGNs, UV emission is blocked at the inner surface of the surrounding dust shell, but X-rays can penetrate deeply into the dust to produce X-ray dissociation regions (XDRs; Maloney, Holllenbach, & Tielens 1996). In XDRs, locally generated UV photons, such as Lyman-Werner band H_2 emission and Lyα emission, can ionize some species with ionization potential less than 10–11 eV (notably carbon and iron), but the emitting volume is dominated by largely neutral gas, which causes XDRs essentially always to have LINER-type spectra (P. Maloney 2001, in preparation). A buried AGN can thus explain the observed LINER-type optical emission.

However, in practical cases, some star formation activity may very well be present at the surface of galaxies even when buried AGNs are energetically dominant, as we infer for UGC 5101. In such a case, due to the susceptibility of optical emission to dust extinction, the optical spectral diagnostics are likely to be dominated by this surface star formation emission. The star formation activity could be responsible for LINER-type optical emission via shocks or might even alter the optical emission to an H II region type. It is important to note that narrow-line emission from high-excitation clouds characteristic of Seyfert galaxy spectra that are observed to be produced along the axes of nuclear dust tori would not contribute substantially at any wavelength in the case of a buried AGN.

5. SUMMARY

We have found evidence for the presence of an energetically dominant, buried AGN in the ULIRG UGC 5101, which is characterized by a cool far-infrared color and a LINER optical spectrum. This finding seems contrary to the currently established view, based on *ISO* data, that such objects are powered by star formation. Two other LINER ULIRGs also show evidence for energetically dominant buried AGNs, and we therefore conclude that at least some fraction of LINER ULIRGs are powered by buried AGNs.

We are grateful to J. Rayner and B. Golisch for their support before and during the observing run. Research in infrared astronomy at NRL is supported by the Office of Naval Research. P. R. M. is supported by the NSF under grant AST 99-00871. This research has made use of the NASA/IPAC Extragalactic Database (NED), which is operated by the Jet Propulsion Laboratory, California Institute of Technology, under contract with the National Aeronautics and Space Administration.

REFERENCES

Alonso-Herrero, A., Ward, M. J., & Kotilainen, J. K. 1997, MNRAS, 288, 977
Barger, A. J., Cowie, L. L., & Richards, E. A. 2000, AJ, 119, 2092
Blain, A. W., Kneib, J.-P., Ivison, R. J., & Smail, I. 1999a, ApJ, 512, L87
Blain, A. W., Smail, I., Ivison, R. J., & Kneib, J.-P. 1999b, MNRAS, 302, 632
Cox, M. J., Eales, S. A. E., Alexander, P., & Fitt, A. J. 1988, MNRAS, 235, 1227
Crawford, T., Marr, J., Partridge, B., & Strauss, M. A. 1996, ApJ, 460, 225
Dudley, C. C. 1999, MNRAS, 307, 553
Dudley, C. C., & Wynn-Williams, C. G. 1997, ApJ, 488, 720
Fischer, J. 2000, in *ISO* Beyond the Peaks, ed. A. Salama, M. F. Kessler, K. Leech, & B. Schulz (ESA SP-456; Noordwijk: ESA), 239
Genzel, R., & Cesarsky, C. J. 2000, ARA&A, 38, 761
Genzel, R., et al. 1998, ApJ, 498, 579
Imanishi, M., & Dudley, C. C. 2000, ApJ, 545, 701
Lonsdale, C. J., Smith, H. E., & Lonsdale, C. J. 1995, ApJ, 438, 632
Lutz, D., et al. 1996, A&A, 315, L269
Lutz, D., Veilleux, S., & Genzel, R. 1999, ApJ, 517, L13
Maloney, P. R., Hollenbach, D. J., & Tielens, A. G. G. M. 1996, ApJ, 466, 561
Mouri, H., Kawara, K., Taniguchi, Y., & Nishida, M. 1990, ApJ, 356, L39
Nakagawa, T., Kii, T., Fujimoto, R., Miyazaki, T., Inoue, H., Ogasaka, Y., Arnaud, K., & Kawabe, R. 1999, in IAU Symp. 186, Galaxy Interactions at Low and High Redshift, ed. J. E. Barnes & D. B. Sanders (Dordrecht: Kluwer), 341
Pendleton, Y. J., Sandford, S. A., Allamandola, L. J., Tielens, A. G. G. M., & Sellgren, K. 1994, ApJ, 437, 683
Predehl, P., & Schmitt, J. H. M. M. 1995, A&A, 293, 889
Rigopoulou, D., Spoon, H. W. W., Genzel, R., Lutz, D., Moorwood, A. F. M., & Tran, Q. D. 1999, AJ, 118, 2625
Roche, P. F., Aitken, D. K., Smith, C. H., & Ward, M. J. 1991, MNRAS, 248, 606
Sanders, D. B., & Mirabel, I. F. 1996, ARA&A, 34, 749
Sanders, D. B., Soifer, B. T., Elias, J. H., Madore, B. F., Matthews, K., Neugebauer, G., & Scoville, N. Z. 1988a, ApJ, 325, 74
Sanders, D. B., Soifer, B. T., Elias, J. H., Neugebauer, G., & Matthews, K. 1988b, ApJ, 328, L35
Scoville, N. Z., et al. 2000, AJ, 119, 991
Shure, M. A., Toomey, D. W., Rayner, J. T., Onaka, P., & Denault, A. J. 1994, Proc. SPIE, 2198, 614
Smith, H. E., Lonsdale, C. J., & Lonsdale, C. J. 1998, ApJ, 492, 137
Soifer, B. T., Sanders, D. B., Madore, B. F., Neugebauer, G., Danielson, G. E., Elias, J. H., Lonsdale, C. J., & Rice, W. L. 1987, ApJ, 320, 238
Soifer, B. T., et al. 2000, AJ, 119, 509
Sopp, H. M., & Alexander, P. 1991, MNRAS, 251, 112
Spoon, H. W. W., Keane, J. V., Tielens, A. G. G. M., Lutz, D., & Moorwood, A. F. M. 2001, A&A, 365, L353
Taniguchi, Y., Yoshino, A., Ohyama, Y., & Nishiura, S. 1999, ApJ, 514, 660
Tokunaga, A. T. 2000, in Allen's Astrophysical Quantities, ed. A. N. Cox (4th ed.; New York: AIP), 143
Tokunaga, A. T., Sellgren, K., Smith, R. G., Nagata, T., Sakata, A., & Nakada, Y. 1991, ApJ, 380, 452
Tran, Q. D., et al. 2001, ApJ, 552, 527
Veilleux, S., Kim, D.-C., & Sanders, D. B. 1999a, ApJ, 522, 113
Veilleux, S., Sanders, D. B., & Kim, D.-C. 1999b, ApJ, 522, 139